

A multi-objective approach to the design of low thrust space trajectories using optimal control

Michael Dellnitz*, Sina Ober-Blöbaum†, Marcus Post‡,
Oliver Schütze§, Bianca Thiere*

August 25, 2009

Abstract

In this article, we introduce a novel *three-step approach* for solving optimal control problems in space mission design. We demonstrate its potential by the example task of sending a group of spacecraft to a specific Earth L_2 Halo orbit. In each of the three steps we make use of recently developed optimization methods and the result of one step serves as input data for the subsequent one.

Firstly, we perform a global and multi-objective optimization on a restricted class of control functions. The solutions of this problem are (Pareto-)optimal with respect to ΔV and flight time. Based on the solution set, a compromise trajectory can be chosen suited to the mission goals. In the second step, this selected trajectory serves as initial guess for a direct local optimization. We construct a trajectory using a more flexible control law and, hence, the obtained solutions are improved with respect to control effort. Finally, we consider the improved result as a reference trajectory for a formation flight task and compute trajectories for several spacecraft such that these arrive at the Halo orbit in a prescribed relative configuration.

The strong points of our three-step approach are that the challenging design of good initial guesses is handled numerically by the global optimization tool and afterwards, the last two steps only have to be performed for *one* reference trajectory.

Keywords: space mission design, low thrust propulsion, three body problem, multi-objective optimization, Pareto set, optimal control, formation flight.

PACS: 95.10.Ce, 02.60.Pn, 45.20.Jj, 45.80.+r, 45.10.Db

*Faculty of Computer Science, Electrical Engineering and Mathematics, University of Paderborn, D-33095 Paderborn, Germany, {dellnitz, thiere}@math.upb.de

†Control and Dynamical Systems, MC 107-81, California Institute of Technology, Pasadena, CA 91125, USA, sinaob@cds.caltech.edu

‡TU München, Zentrum Mathematik, Boltzmannstr. 3, D-85747 Garching bei München, Germany, marcus.post@ma.tum.de

§CINVESTAV-IPN, Computer Science Department, Mexico City, Mexico, schuetze@cs.cinvestav.mx

1 Introduction

Over the last years dynamical system techniques have been developed for the design of energy-efficient spacecraft trajectories. These methods exploit the natural dynamics of the system and often result in trajectories that are close to invariant manifolds. Famous space missions using dynamical system techniques were for instance the Japanese *Hiten mission* in the 90's and the *Genesis Discovery Mission* which was a solar-wind sample return mission between 2001 and 2004. The Hiten mission marked the first use of a weak stability boundary transfer – a mathematical concept which Belbruno introduced to design trajectories for space missions (see e.g. [Belbruno and Miller (1993)] for more mathematical details). The delicate heteroclinic dynamics employed by the Genesis mission illustrates again the need to study the three body problem (3BP) using dynamical systems theory (see e.g. [Howell et al. (1997), Koon et al. (1999), Dellnitz et al. (2001), Gómez et al. (2001)]).

There are different ways of finding good and optimal trajectories for missions without the consideration of invariant manifolds. Promising results in using the strategy for low thrust transfer are e.g. given in [Koon et al. (2001), Dellnitz et al. (2006b), Garcia and Gómez (2007)], and more recently new techniques are developed for instance by [Leiva and Briozzo (2008), Mingotti et al. (2009), Pergola et al. (2009)]. Another approach is to consider hybrid optimal control problems which attract increasing interest. For a description of such a problem see for instance [Conway et al. (2007), Vasile (2009)] and references therein.

Our approach is a combination of using dynamical system theory and (multi-objective) optimization. However, one major drawback is that the high efficiency in fuel consumption is relativized by long flight times. Thus, a typical trade-off in space mission design is to apply more thrust (and, in turn, increase the cost of the resulting mission) to obtain shorter mission times (see e.g. [Coverstone-Carroll et al. (2000), Lee et al. (2005), Vasile et al. (2006), Schütze et al. (2008b), Schütze et al. (2008c), Vavrina and Howell (2008)]). A natural mathematical framework to deal with such trade-offs is to describe the task as a (global) *multi-objective optimization problem (MOP)*. Global optimization methods are well suited for more or less detailed preselections of promising trajectories as a *first guess*. Typically, in a second step this first guess is then subject to a local optimization method with a more detailed model and a more flexible control law.

While all the works mentioned above dealing with the multi-objective trajectory design address the computation of first guess solutions, we propose here a particular composition of optimization methods to accomplish the trajectory design. We introduce a novel three-step approach for solving optimal control problems in space mission design. In each of the three steps we make use of recently developed optimization methods and the result of one step serves as input data for the next one (see Figure 1 for a schematically overview).

To be more precise, in the first step we perform a global and multi-objective optimization on a restricted class of control functions by a set-oriented method. The solutions of

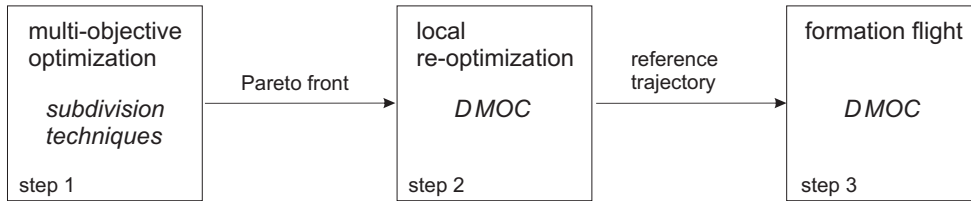


Figure 1: Novel three-step approach (schematically)

this problem are (Pareto-)optimal with respect to the two objectives ΔV and flight time. Based on this information, a mission designer can choose a compromise trajectory suited to the mission goals. In the second step this selected trajectory serves as initial guess for a direct local optimization method called DMOC (Discrete Mechanics and Optimal Control). By means of DMOC we construct a trajectory using a more flexible control law and, hence, the obtained solutions are improved with respect to control effort. Finally, we consider the DMOC result as a reference trajectory for a formation flight task and compute trajectories for several spacecraft – again by DMOC – such that these arrive at the Halo orbit in a prescribed relative configuration.

We demonstrate the efficiency of the combined optimization approach by a numerical example and point out that the decision on suitable trajectories for a formation flight can already be based on the data that are obtained in a computational cheap way in the first step. Then, the time-consuming local optimization used for a more flexible control law and the formation flight only has to be carried out for one selected solution.

Global multi-objective optimization While in the single-objective case the solution is typically – i.e. under mild regularity assumptions – given by *one* point, the solution set of an MOP consisting of k objectives typically forms a $(k - 1)$ -dimensional object [Hillermeier (2001)]. This set is called the *Pareto set* (see [Pareto (1971)]) or the set of optimal compromises. Over the last years quite a few methods from different fields have been suggested for the solution of MOPs (see e.g. [Miettinen (1999), Coello Coello et al. (2007), Deb (2001), Hillermeier (2001)] and references therein). Within this study we use multi-objective subdivision techniques [Dellnitz et al. (2005)] which are state of the art for the numerical treatment of moderate dimensional MOPs such as the one considered in Section 3.1.

In the context of this article we want to stress that the knowledge of the *entire* Pareto set of the bi-objective problem (minimization of flight time and fuel consumption) can help a mission designer to decide which optimal compromise to take. Questions like ‘how much time do we save if we use a bit more fuel during the mission’ can be quickly answered by looking at a graphical representation of the Pareto front, i.e. the image of the Pareto set.

Local single-objective optimal control Although the benefits of a global multi-objective optimization for decision making are sketched above, the computational burden of solving such optimization problems is relatively high. Hence, the underlying models are typically somehow restricted. As mentioned before, a standard approach is to select a compromise by means of the restricted model and then locally (re-)optimize the corresponding trajectory by a single-objective local method with a more detailed model.

We give a short overview of local optimal control methods. In principle, there exist indirect and direct local optimal control methods. In our contribution we focus on direct methods. Some well-known direct methods are shooting techniques (see for instance [Kraft (1985), Hicks and Ray (1971), Stoer and Bulirsch (1993)]), multiple shooting (see [Deuffhard (1974), Bock and Plitt (1984), Leineweber et al. (2003)]), and collocation methods (see e.g. [Biegler (1984), von Stryk (1993)]). These methods rely on a direct integration of the associated ordinary differential equations, see also [Betts (1998)] and [Binder et al. (2001)] for an overview of the current state of the art. In contrast to these tools the recently developed DMOC (*Discrete Mechanics and Optimal Control*) [Junge et al. (2005), Ober-Blöbaum (2008)] is based on the discretization of the variational structure of the mechanical system directly. In the context of variational integrators (see for instance [Marsden and West (2001)]), the discretization of the Lagrange-d'Alembert principle leads to structure preserving time stepping equations which serve as equality constraints for the resulting finite dimensional nonlinear optimization problem. This problem can be solved by standard nonlinear optimization techniques such as *Sequential Quadratic Programming (SQP)* (see e.g. [Gill et al. (1997), Gill et al. (2000), Powell (1978), Han (1976)]) leading to local optimal solutions dependent on the initial guess in use.

Formation flight With the described methods on-hand, we are able to compute fuel- and time-efficient reconfiguration maneuvers of formation flying spacecraft in the following way: After having identified a promising reference trajectory by the composition of global multi-objective optimization and local optimal control methods, we determine a reconfiguration maneuver of a group of spacecraft along that trajectory.

Work on formation flying spacecraft has been motivated by the ESA mission DARWIN¹. The aim of DARWIN is to detect Earth-like planets by interferometric measurements ('nulling interferometry') using a formation of spacecraft as a high performance telescope. That means, the huge size of a single telescope necessary for managing such a task is overcome by using accurately light collectors which will redirect light to the central hub spacecraft. Important mission goals are the formation-keeping and reconfiguration of the spacecraft as well as its long operation time. The latter is dealt with by using low thrust engines with their high specific impulse.

Different control methodologies have been investigated in work of several authors, see for instance [Howell and Marchand (2003), Marchand and Howell (2003)] as well as

¹ http://www.esa.int/esaSC/120382_index_0_m.html

[Marchand et al. (2005)] and references therein. Here, the goal is to keep a predefined formation along a Halo orbit around the Lagrange points L_1 or L_2 . Different to the work by these authors, we are only interested in the optimal reconfiguration of formation flying spacecraft like in [Junge and Ober-Blöbaum (2005)], i.e. the spacecraft reconfigure from an initial configuration to a prescribed target configuration. During the reconfiguration the spacecraft have to fulfill a desired minimal distance (to avoid collisions) and maximal distance (to ensure communication ability). For the reconfiguration we again use the local optimal control method DMOC.

A numerical example In our example, we compute energy- and time-efficient low thrust trajectories for a formation of spacecraft which arrives at an Earth L_2 Halo orbit. For this purpose, we consider a controlled version of the **Circular Restricted Three Body Problem** (CCRTBP) with Sun and Earth as the primaries. Of course, there exist more detailed models for the design of spacecraft trajectories. However, the main goal of our example is to present our new three-step approach. Additionally, the three body problem has the advantage that many of its properties are already well understood.

Organization of the article The remainder of this article is organized as follows: In Section 2, we state the background required for the understanding of the sequel. That is, we present some basic facts on the standard three body problem and introduce the restricted control term which we utilize for the global optimization. Further, we state the required background on multi-objective optimization and one state of the art algorithm for the numerical treatment of such problems. Finally, we introduce DMOC, the local optimization method we use to compute the refined trajectories. In Section 3, we present the three-step optimization process and demonstrate its applicability to a particular example, the CCRTBP. To be more precise, we compute a set of ‘optimal’ trajectories – according to the simplified system – from Earth to an Earth L_2 Halo orbit (Section 3.1), and we refine them in the next step using DMOC (Section 3.2). To complete the example, we compute reconfiguration maneuvers where we choose the obtained solutions as reference trajectories (Section 3.3). Finally, we draw some conclusions and state possible directions for future work in Section 4.

2 Model description and optimization methods

In this section we briefly summarize the background required for this work. Thereby, we start with a description of the **Circular Restricted Three Body Problem** (CRTBP) and emphasize the extension to a controlled problem (CCRTBP). Using the CCRTBP we are able to compute reachable sets which will be of use for the forthcoming optimization. Afterwards, the basic definition of the concept of multi-objective optimization are given followed by the description of the subdivision techniques we are using. At the end of this section we introduce the concept of the local optimal control method DMOC.

2.1 The Controlled Circular Restricted Three Body Problem

The Spatial Circular Restricted Three Body Problem As alluded to in the Introduction, we consider the (*spatial*) *circular restricted three body problem (CR3BP)* with Sun and Earth as main bodies, with masses m_1 and m_2 , respectively. The mass of the third body – typically an asteroid, a comet, a spacecraft, or just a particle – is assumed to be negligible. For instance [McGehee (1969)] and [Koon et al. (2000)] noticed the importance of this model for modeling the dynamics of a space mission between different planets.

Let us briefly recall the basics of this model – for a more detailed exposition we refer to [Szebehely (1967), Meyer and Hall (1992), Belbruno (2004), Gómez et al. (2001), Abraham and Marsden (1978)]. The CR3BP models the motion of a particle in the gravitational field of two bodies like e.g. Sun and Earth. These two primaries move in a plane counterclockwise on circles about their common center of mass with the same constant angular velocity. The third body does not influence the motion of the primaries while it is only influenced by their gravitational forces. In a normalized rotating coordinate system the origin is the center of mass and the two primaries are fixed on the x_1 -axis at $(-\mu, 0, 0)$ and $(1 - \mu, 0, 0)$, respectively, where $\mu = m_1/(m_1 + m_2)$. For the three body problem Sun-Earth-spacecraft we use $\mu_{SE} = 3.04041307864 \cdot 10^{-6}$.

The equations of motion for the spacecraft with position (x_1, x_2, x_3) in rotating coordinates are given by

$$\begin{aligned}\ddot{x}_1 - 2\dot{x}_2 &= \Omega_{x_1}(x_1, x_2, x_3), \\ \ddot{x}_2 + 2\dot{x}_1 &= \Omega_{x_2}(x_1, x_2, x_3), \\ \ddot{x}_3 &= \Omega_{x_3}(x_1, x_2, x_3),\end{aligned}\tag{1}$$

where

$$\Omega(x_1, x_2, x_3) = \frac{x_1^2 + x_2^2}{2} + \frac{1 - \mu}{r_1} + \frac{\mu}{r_2} + \frac{\mu(1 - \mu)}{2}$$

and

$$r_1 = \sqrt{(x_1 + \mu)^2 + x_2^2 + x_3^2}, \quad r_2 = \sqrt{(x_1 - 1 + \mu)^2 + x_2^2 + x_3^2}.$$

Here, the subscripts of Ω denote partial differentiation in the respective variable, and r_1, r_2 are the distances from the particle to the Sun and Earth, respectively.

The equations (1) have a first integral, the *Jacobi integral*, which is given by

$$C(x_1, x_2, x_3, \dot{x}_1, \dot{x}_2, \dot{x}_3) = -(\dot{x}_1^2 + \dot{x}_2^2 + \dot{x}_3^2) + 2\Omega(x_1, x_2, x_3).\tag{2}$$

The five-dimensional manifold of constant values of the Jacobi constant are an indicator of the type of global dynamics possible for a particle in the CRTBP and are invariant under the flow of (1). Their projection onto position space, *Hill's region*, determines the allowed region for the motion of the spacecraft (cf. Figure 2). In our example we consider

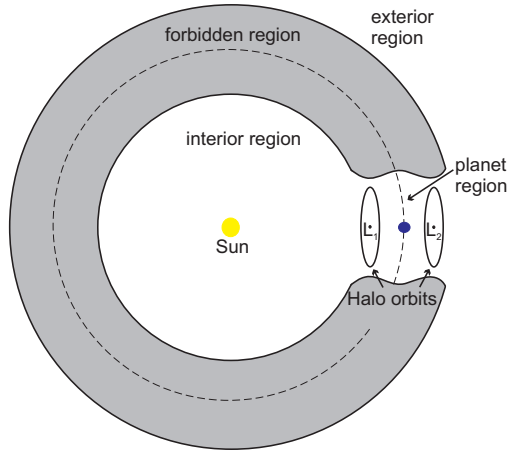


Figure 2: Projection of an energy surface onto the x_1x_2 -plane (schematic) for a value of the Jacobi integral for which the spacecraft is able to transit between the exterior and the interior region.

a target with a Jacobi constant given by $C = 3.0005$.

The system possesses five equilibrium points (the *Lagrange points*) – the collinear points L_1, L_2 and L_3 on the x_1 -axis and the equilateral points L_4 and L_5 . It is known (see e.g. [Barden et al. (1997)] and [Dichmann et al. (2003)]) that there exist families of periodic orbits – the so-called *Halo orbits* around the Lagrange points L_1 and L_2 . Those Halo orbits of the spatial problem are of interest to us. In [Junge et al. (2002)] further references are given that these orbits are especially suited for space missions for single and multiple spacecraft. For multiple spacecraft missions, key aspects are for instance the movement along a trajectory in a special formation or the arrival at the destination with a prescribed relative position. Whereas in [Junge et al. (2002)] a heuristic suboptimal control law is developed for keeping a formation near the Halo orbit we tackle the problem in such a way that the spacecraft build a given formation at arrival time. Moreover, we employ a sophisticated global and local optimization method to determine an optimal control law.

On the choice of the model The CR3BP serves as our test model since its dynamics describes the motion of a spacecraft and it is well-understood (see for instance [Szebehely (1967), Farquhar (1970), Richardson (1980), Belbruno and Marsden (1997)]). Some of the key features of the CR3BP which ease the application of our three-step algorithm are: the CR3BP is autonomous and it possesses the Jacobi integral and periodic orbits around the Lagrange points with their invariant manifolds. Going one step further, near the Lagrange points L_1 and L_2 in the CR3BP there exist artificial equilibrium points. Around those points it is possible to find periodic orbits which are also of interest to mission planners, see e.g. [Baig and McInnes (2009)].

Nevertheless, our algorithm can also be applied to more general problems. For space mission design the exploration of the elliptic restricted three body problem (ER3BP) can be worthwhile (see e.g. [Szebehely (1967), Kechichian (2002), Gawlik et al. (2009)]). The ER3BP is a natural generalization of the CR3BP which is no longer autonomous and also the other mentioned key features are not valid. That is why we stick to the CR3BP for the context of this contribution which we now extend by a control.

A heuristic control For current mission concepts, like the ESA interplanetary mission *BepiColombo*² or the DARWIN mission ion propulsion systems are being considered that continuously exert a small force on the spacecraft (“low-thrust propulsion”). This new engine type was already successfully applied in previous missions such as *Smart I*.³ However, the previously introduced circular restricted three body problem (1) does not model this continuous thrusting capability and thus the model needs to be enhanced by a suitably defined control term. As in [Dellnitz et al. (2006b)], we restrict our considerations to the special case of a control force whose direction is defined by the velocity of the spacecraft. The reason is that an acceleration parallel to the velocity vector yields a maximum instantaneous impact onto the kinetic energy of the spacecraft. However, this does not imply a globally optimal impact [Tang and Conway (1995)] but serves as heuristic to reduce the space of control functions in the global part of the latter optimization procedure. The locally maximal impact can be seen by the time derivative of kinetic energy which solely depends on the dot product of the velocity of the spacecraft and its acceleration if the mass is assumed to be constant (see [Gerthsen and Vogel (1993)]).

The control term which has to be included into the model is therefore parametrized by a single real value u , determining the magnitude of the control acceleration. We do not take into account that the mass of the spacecraft changes during its flight since in our modeling the spacecraft has negligible mass. The only effect would be that the same acceleration u can be achieved by less driving force if the mass decreases over time. This would allow to employ a higher upper bound for u at a later time which means that we maintain a conservative estimate for this upper bound.

The velocity vector of the spacecraft has to be viewed with respect to the inertial coordinate system and not the rotating one. In view of this, one is lead to the following control system, modeling the motion of the spacecraft under the influence of its low thrust propulsion engines in rotating coordinates (cf. Figure 3):

$$\ddot{x} + 2\dot{x}^\perp = \nabla\Omega(x) + u \frac{\dot{x} + \omega x^\perp}{|\dot{x} + \omega x^\perp|}. \quad (3)$$

Here, $u = u(t) \in [u_{\min}, u_{\max}] \subset \mathbb{R}$ denotes the magnitude of the control force, $x = (x_1, x_2, x_3)$, $x^\perp = (-x_2, x_1, 0)$ and $\omega = 1$ is the common angular velocity of the primaries in the x_1x_2 -plane.

²<http://sci.esa.int/science-e/www/area/index.cfm?fareaid=30>

³<http://sci.esa.int/science-e/www/area/index.cfm?fareaid=10>

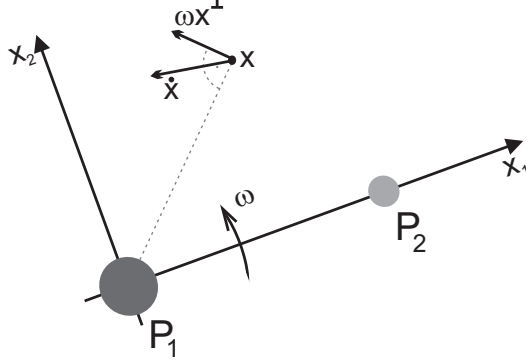


Figure 3: The velocity of the spacecraft with respect to the inertial frame is given by $\dot{x} + \omega x^\perp$. Since the rotation of the primaries takes places in the x_1x_2 -plane, only the projection onto that plane is illustrated.

Reachable sets Obviously, every solution of (1) is also a solution of (3) for the control function $u \equiv 0$. We are going to exploit this fact in order to generalize the standard manifold approach to the case of controlled three body problems. Instead of computing the relevant time-backward invariant manifolds of the periodic Halo orbit, we compute certain time-backward *reachable sets* (see e.g. [Colonius and Kliemann (2000)]), i.e. sets in phase space that can be accessed by the spacecraft when employing a certain control function.

We denote by $\phi(t, z, u)$ the solution of the control system (3) for a given initial point $z = (x, \dot{x})$ in the phase space Z at $t_0 = 0$ and a given admissible control function $u \in \mathcal{U} = \{u : \mathbb{R} \rightarrow [u_{\min}, u_{\max}], u \text{ admissible}\}$. Here $u_{\min}, u_{\max} \in \mathbb{R}$ are predetermined bounds on the magnitude of the control force, and the attribute "admissible" alludes to the fact that only a certain subset of functions is allowed. Both, the bounds and the set of admissible control functions will be determined by the design of the thrusters. For example, the set of admissible control functions could be the set of piecewise constant functions, where the minimal length of an interval on which the function is constant is determined by how fast the magnitude of the accelerating force can be changed within the thrusters.

For a set S in phase space Z (S being an element of the power set $\mathbb{P}(Z)$) and a given function $\tau : S \times \mathcal{U} \rightarrow \mathbb{R}$, we call $\mathcal{R} : \mathbb{P}(Z) \times (S \times \mathcal{U} \mapsto \mathbb{R}) \mapsto \mathbb{P}(Z)$ with

$$\mathcal{R}(S, \tau) = \{\phi(\tau(z, u), z, u) \mid u \in \mathcal{U}, z \in S\}$$

the set which is (τ) -reachable from S . Later on, we choose $\tau(x, u)$ in such a way that the reachable sets are contained in an intersection plane close to Earth. In this way, the dimension of the reachable set is reduced by one.

2.2 Multi-objective optimization

For the global multi-objective optimization process we consider continuous MOPs of the form

$$\min_x G(x), \quad (4)$$

where $G : Q \subset \mathbb{R}^n \rightarrow \mathbb{R}^k$ is a vector of objective functions

$$G(x) = (g_1(x), \dots, g_k(x)),$$

and each objective $g_i : Q \rightarrow \mathbb{R}$ is continuous. Further, we assume that each parameter x_i , $i = 1, \dots, n$, is restricted to a certain range $a_i \leq x_i \leq b_i$ leading to the domain Q given by

$$Q = \{x \in \mathbb{R}^n : a_i \leq x_i \leq b_i, i = 1, \dots, n\}. \quad (5)$$

The optimality of an MOP is defined by the concept of *dominance* which dates back over one century and was first introduced by Pareto [Pareto (1971)]. For the test of dominance the following definitions are necessary.

DEFINITION 2.1 (a) Let $v, w \in \mathbb{R}^k$. Then the vector v is *less than* w ($v <_p w$), if $v_i < w_i$ for all $i \in \{1, \dots, k\}$. The relation \leq_p is defined analogously.

(b) A vector $y \in \mathbb{R}^n$ is *dominated* by a vector $x \in \mathbb{R}^n$ ($x \prec y$) with respect to (4) if $G(x) \leq_p G(y)$ and $G(x) \neq G(y)$, else y is called non-dominated by x .

(c) A point $x \in Q$ is called (*Pareto*) *optimal* or a *Pareto point* if there is no $y \in Q$ which dominates x .

The set of all Pareto optimal solutions is called the *Pareto set*, denoted by P_Q . The image $G(P_Q)$ of the Pareto set is called the *Pareto front*. P_Q forms typically – i.e. under mild regularity assumptions on the MOP – a $(k - 1)$ -dimensional object, i.e., a curve or a set of curves for bi-objective models as considered here.

For the approximation of the Pareto set of a given MOP there exist several classes of algorithms. For instance, a variety of mathematical programming techniques exploit the gradient information of the model (if provided). Such methods include scalarization techniques, i.e., the MOP is transformed into a sequence of scalar optimization problems (see [Miettinen (1999), Fliege and Svaiter (2000), Das and Dennis (1998)] and references therein), or multi-objective continuation methods ([Hillermeier (2001)]). In general, those approaches are very efficient in finding single solutions or even sets of solutions but may fail to find the entire (global) Pareto set.

In contrast, there exist other global methods which work without gradient information and are capable of finding the entire solution set but offer in turn much slower convergence rates than the local approaches. These are for instance multi-objective evolutionary algorithms (MOEAs) or subdivision techniques. For a general purpose of algorithms of MOEAs we refer to [Deb (2001), Coello Coello et al. (2007)] and references therein. A characterization of MOEAs specialized on space mission design can be

found in [Coverstone-Carroll et al. (2000), Lee et al. (2005), Vasile et al. (2006)] as well as [Schütze et al. (2008c)]. An introduction of how subdivision techniques work is given in the next subsection.

As a logical consequence, there exist a variety of hybrid (or memetic) algorithms, i.e., algorithms which hybridize MOEAs with local search strategies. In such a way one obtains algorithms which are global and robust and offer a reasonable overall performance. Multi-objective memetic strategies specialized on space mission design can be found in [Maddock and Vasile (2008), Vavrina and Howell (2008), Vasile (2009)]. Note that, for a memetic strategy *one* fidelity of the model is required, and this fidelity should not be too low in order to tap the potential of the local search procedure.

Instead of the use of memetic strategies, we propose here to compute the Pareto set in two stages: first, subdivision techniques are used to compute the Pareto set \mathcal{P} of a reduced model, and then, the set \mathcal{P} serves as initial guess for the local search procedure DMOC using a model with higher fidelity.

2.3 Multi-objective subdivision techniques

The subdivision techniques described in [Schütze et al. (2003)] and [Dellnitz et al. (2005)] are set-oriented methods and have been primarily designed for the numerical treatment of MOPs without equality constraints. Algorithms of this type start with the domain Q (see (5)), which constitutes an n -dimensional *box*. This box gets subdivided into a set of smaller boxes, and according to certain conditions it is decided which box could contain a part of the Pareto set and is thus suited for further investigation. The other, unpromising boxes, are discarded from the collection. This process, i.e., subdivision and selection, is performed on the current box collection until the desired granularity of the boxes is reached (which is problem dependent). The approach is of global nature, that is, in principle capable of detecting the entire set of Pareto points, see Figure 4 for an example. The convergence of the underlying abstract algorithm is analyzed in [Dellnitz et al. (2002), Dellnitz et al. (2005)].

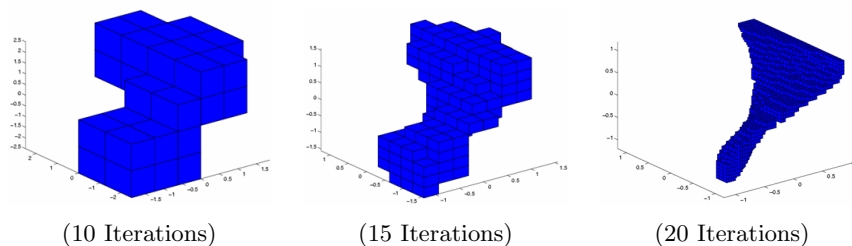


Figure 4: Application of the subdivision algorithm on an MOP $G : Q \subset \mathbb{R}^3 \rightarrow \mathbb{R}^3$, where Q is defined by box-constraints (see [Dellnitz et al. (2005)]). The box collections show different coverings of the Pareto set.

Subdivision algorithms are very effective for the numerical treatment of moderate

dimensional models, and have been used successfully in several applications (see e.g. [Dellnitz et al. (2005), Schütze et al. (2008a), Schütze et al. (2008b)]).

At the end of this section we introduce a local optimization method which is used to optimize the initial guess obtained by the MOP and allows to take a more general control law into account. Furthermore, we are able to design trajectories for all formation flying spacecraft which move close to the locally optimized favorite barycentric trajectory.

2.4 Discrete Mechanics and Optimal Control (DMOC)

In order to locally solve optimal control problems, we use DMOC, a technique that relies on a direct discretization of the variational formulation of the dynamics of the system (see [Junge et al. (2005), Ober-Blöbaum (2008)]). For convenience, we briefly summarize the basic idea.

A mechanical system with configuration space M is to be moved on a curve $x(t) \in M$, $t \in [0, T]$, from a state (x^0, \dot{x}^0) to a state (x^T, \dot{x}^T) under the influence of a force $f : TM \times U \rightarrow T^*M$, where TM and T^*M are the tangent and cotangent space of the configuration space M , respectively. This force depends on a time dependent control parameter $u(t) \in U$. The curves x and u shall minimize a given objective functional $J : TM \times U \rightarrow \mathbb{R}$

$$J(x, \dot{x}, u) = \int_0^T C(x(t), \dot{x}(t), u(t)) dt \quad (6)$$

with the cost function $C : TM \times U \rightarrow \mathbb{R}$. If $L : TM \rightarrow \mathbb{R}$ denotes the Lagrangian of the system, its motion $x(t)$ satisfies the *Lagrange-d'Alembert principle*, which requires that

$$\delta \int_0^T L(x(t), \dot{x}(t)) dt + \int_0^T f(x(t), \dot{x}(t), u(t)) dt = 0 \quad (7)$$

for all variations δx with $\delta x(0) = \delta x(T) = 0$. This principle leads to a system of second order differential equations denoted as the *forced Euler-Lagrange equations*

$$\frac{d}{dt} \frac{\partial}{\partial \dot{x}} L(x, \dot{x}) - \frac{\partial}{\partial x} L(x, \dot{x}) = f(x, \dot{x}, u). \quad (8)$$

The minimization of (6) subject to the equations (8) and initial and final state conditions constitutes the optimal control problem in the continuous setting.

Using a global discretization of the states and the controls one obtains the *discrete Lagrange-d'Alembert principle* which specifies equality constraints for the resulting finite dimensional nonlinear optimization problem as described next.

Discretization We replace the state space TM by $M \times M$ and consider the grid $\Delta t = \{t_k = kh \mid k = 0, \dots, N\}$, $Nh = T$, where N is a positive integer and h the step size. We replace a path $x : [0, T] \rightarrow M$ by a *discrete path* $x_d : \{t_k\}_{k=0}^N \rightarrow M$, where we view $x_k = x_d(kh)$ as an approximation to $x(kh)$ [Marsden and West (2001), Ober-Blöbaum (2008)]. Similar, we replace the control path $u : [0, T] \rightarrow U$ by a discrete one. To this end we

consider a refined grid $\Delta\tilde{t}$, generated via a set of control points $0 \leq c_1 < \dots < c_s \leq 1$ as $\Delta\tilde{t} = \{t_{k\ell} = t_k + c_\ell h \mid k = 0, \dots, N-1; \ell = 1, \dots, s\}$. With this notation the *discrete control path* is defined to be $u_d : \Delta\tilde{t} \rightarrow U$. We define the *intermediate control samples* u_k on $[t_k, t_{k+1}]$ as $u_k = (u_{k1}, \dots, u_{ks}) \in U^s$ to be the values of the control parameters guiding the system from $x_k = x_d(t_k)$ to $x_{k+1} = x_d(t_{k+1})$, where $u_{kl} = u_d(t_{kl})$ for $l \in \{1, \dots, s\}$.

Via an approximation of the action integral in (7) by a *discrete Lagrangian* $L_d : M \times M \rightarrow \mathbb{R}$,

$$L_d(x_k, x_{k+1}) \approx \int_{kh}^{(k+1)h} L(x(t), \dot{x}(t)) dt, \quad (9)$$

and *discrete forces*

$$f_k^- \cdot \delta x_k + f_k^+ \cdot \delta x_{k-1} \approx \int_{kh}^{(k+1)h} f(x(t), \dot{x}(t), u(t)) \cdot \delta x(t) dt, \quad (10)$$

where the left and discrete forces f_k^\pm now depend on (x_k, x_{k+1}, u_k) we obtain the *discrete Lagrange-d'Alembert principle* (11). This requires to find discrete paths $\{x_k\}_{k=0}^N$ such that for all variations $\{\delta x_k\}_{k=0}^N$ with $\delta x_0 = \delta x_N = 0$, one has

$$\delta \sum_{k=0}^{N-1} L_d(x_k, x_{k+1}) + \sum_{k=0}^{N-1} (f_k^- \cdot \delta x_k + f_k^+ \cdot \delta x_{k+1}) = 0, \quad (11)$$

which is equivalent to the *forced discrete Euler-Lagrange equations*

$$D_2 L_d(x_{k-1}, x_k) + D_1 L_d(x_k, x_{k+1}) + f_{k-1}^+ + f_k^- = 0, \quad k = 1, \dots, N-1, \quad (12)$$

where D_i denotes the derivative w.r.t. the i -th slot. In the same manner we obtain via an approximation of the objective functional (6) the *discrete objective functional* $J_d(x_d, u_d)$, such that we can formulate the *Discrete Constrained Optimization Problem* as

$$\min_{x_d, u_d} J_d(x_d, u_d) = \sum_{k=0}^{N-1} C_d(x_k, x_{k+1}, u_k) \quad (13)$$

subject to the discretized boundary constraints and the discrete Euler-Lagrange equations (12). This is a nonlinear optimization problem with equality constraints, which can be solved by standard optimization methods like SQP. Optionally, we can also include inequality constraints on states and controls. Due to the local nature of SQP methods a good initial guess is essential for the convergence of the algorithm. These are provided by the solutions resulting from the global scheme described before.

So far, DMOC has been successfully applied to problems in space mission design (see e.g. [Junge and Ober-Blöbaum (2005), Dellnitz et al. (2006a), Junge et al. (2006)]) and robotics (see for instance [Kanso and Marsden (2005), Leyendecker et al. (2007)] as well as [Kobilarov et al.(2007)]).

Numerical properties In contrast to other methods, DMOC is based on the discretization of the variational principle, rather than a discretization of the ordinary differential equations. In [Marsden and West (2001)] a detailed analysis of integrators resulting from this discrete variational approach is given. These integrators are symplectic-momentum preserving, i.e. the symplectic structure and the momentum maps corresponding to symmetry groups are preserved for the discrete solution. Besides exact momentum map preservation, these properties also lead to good energy behavior of the system even for large time steps, i.e. the energy decays or grows in a realistic way without artificial damping resulting from numerical errors. Taking control forces into account, similar structural properties of the continuous solution are preserved for the discrete solution provided by DMOC. For example, in the presence of symmetry groups in the continuous dynamical system, also along the discrete trajectory the change in momentum maps is consistent with the control forces (see [Ober-Blöbaum (2008)]). Although for the problem under consideration, there is no symmetry group that could directly demonstrate the structure preservation, the use of DMOC leads to a reasonable approximation to the continuous solution, in particular for large step sizes, i.e. a small number of discretization points. However, other optimal control methods like collocation or shooting methods could be used as well (for an overview of these methods we refer to the references given in Section 1).

The order of approximation of the discrete Lagrangian and the discrete forces given in (9) and (10), respectively, determines the order of convergence of the optimal control method. In general, one uses polynomial approximations to the trajectories and numerical quadrature to approximate the integrals. Then, the order of the discrete Lagrangian and the discrete forces is given by the order of the quadrature rule in use. In [Ober-Blöbaum (2008)] it is shown that a discrete Lagrangian and discrete forces of order κ lead to an optimal control scheme of order κ .⁴ That means, the state and control trajectories as well as the Lagrange multipliers resulting from the Pontryagin Maximum Principle are approximated with an accuracy of $\mathcal{O}(h^\kappa)$. This is in contrast to other schemes, e.g. standard Runge-Kutta or collocation methods, where the approximation of the Lagrange multipliers may be of one or more orders less and is a result of the symplectic nature of the underlying discretization.

A higher number of discretization points improves the accuracy of the discrete solution, but also increases the dimension of the optimization problem the SQP solver has to deal with. Especially for long flight times a high number of discretization points is required to match the desired accuracy of the trajectory. An implementation on configuration level $Q \times Q$ only, rather than on configuration-momentum or configuration-velocity level, leads to a smaller number of optimization parameters and therefore to a smaller number of SQP iterations⁵ compared to collocation methods. Thereby, the optimal trajectory for

⁴Here, smoothness and coercivity of the solution as well as bounded variation of the controls are assumed.

⁵By exploiting the sparse structure of the optimization problem, the number of SQP iterations grows approximately linearly w.r.t. the number of optimization variables.

the configuration and the control forces is determined while the corresponding momenta and velocities are reconstructed.

3 Problem formulation and numerical solution

3.1 Multi-objective optimization and transfer to L_2

In the following subsection, we explain how to compute the best compromises (Pareto set) of trajectories ending in a parametrized reachable set with respect to the objectives ΔV and flight time (TOF). The reachable set is parametrized such that the optimization procedure can be applied directly. In other words, the basic idea is to compute an approximation of a time-backward reachable set of a selected Halo orbit and to perform the multi-objective optimization on all trajectories which end up in this set.

Computing the parametrized reachable set We describe how to parametrize the reachable set in a natural way by two parameters such that it is possible to calculate the corresponding trajectories by only knowing those parameters. Note that, since we consider time-backward reachable sets, each point of the reachable set is the *starting* point for a corresponding trajectory.

For the purpose of global optimization we restrict ourselves to constant control functions with control values $u \in [u_{\min}, u_{\max}]$ as described in (3). The second parameter θ characterizes the target point $P(\theta)$ on the periodic Halo orbit. A natural choice for θ is to select an arbitrary point $P(0) \in \mathbb{R}^6$ on the periodic Halo orbit and to parametrize it by the flow of the CRTBP. That means, $P(\theta) = \phi(\theta, P(0), 0)$ where we denote by $\phi(t, z, u)$ the solution of the control system (3) as before. In this way, the range of θ is between 0 and the period of the orbit (see also Figure 5).

We numerically proceed to associate trajectories with these two parameters as follows. We shift each point of the Halo orbit slightly to the stable manifold and numerically integrate the control system (3) for a fixed u backwards in time. For the integration we use an 8-th order adaptive Runge-Kutta scheme to obtain the result with very high precision.⁶ After each integration step, we check whether the computed trajectory has crossed the plane $\{x_1 = 1 - \mu_{SE}\}$ and, if so, we start Newton's method to determine a point in that plane.

It is important to note that crossing the plane $\{x_1 = 1 - \mu_{SE}\}$ *only* means that the x_1 coordinate of the spacecraft is the same as that of the Earth. All the other coordinates, particularly x_2 and the 3d-velocity, can (theoretically) differ arbitrarily. Although the consideration of special manifolds restricts the set of trajectories obtained, we are aware that the very next step is to include more realistic constraints on the start points of the

⁶For the integration we use an embedded Runge-Kutta scheme with adaptive step size control as implemented in the code DOP853 by Hairer, Nørsett and Wanner, see [Hairer et al. (1993)]. The error tolerance for the adaptive scheme is set to 10^{-12} .

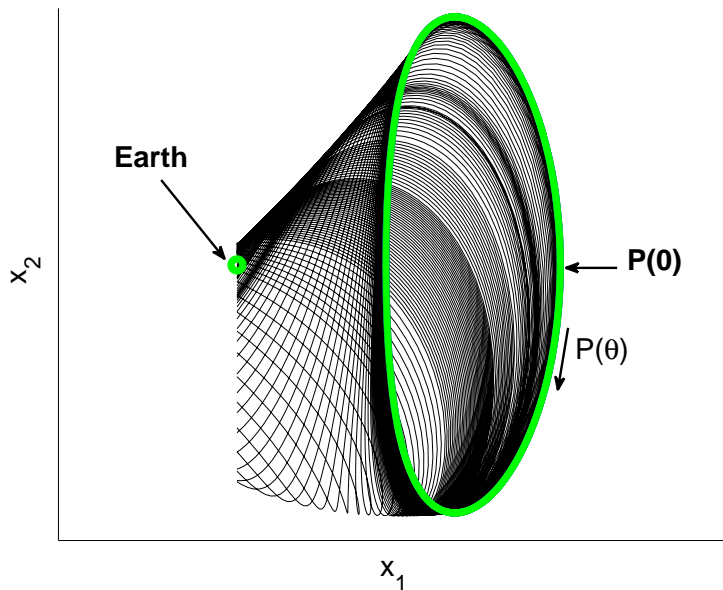


Figure 5: Illustration of the parameter θ of the global MOP for constant control $u = 0$. For any arbitrary selected point $P(0)$ on the periodic Halo orbit the parameter θ uniquely specifies a point $P(\theta)$ on the same orbit with θ between 0 and the period of the orbit. This point – slightly shifted to the stable direction – serves as target for the corresponding trajectory. For $u = 0$ the trajectories are on the stable manifold of the Halo orbit (schematically shown as black lines).

spacecraft. However, we believe that this is a technical issue which in principle can be dealt with within our methodical framework presented in this article.

In our example, we choose $u_{\min} = 0$ mN, $u_{\max} = 800$ mN, and the mass of the spacecraft to be $m_{\text{SC}} = 4000$ kg which only affects the ratio between control force and acceleration in our model. The Halo orbit we consider is determined by its Jacobi constant $C = 3.0005$ and has a period of roughly 0.4778 years, i.e. $\theta \in [0, 0.4778]$ a.

The resulting global MOP All in all, we obtain a family of solutions of the controlled dynamical system which are parametrized by the target point $P(\theta)$ of the specified Halo orbit and by the magnitude of the applied continuous control u . These two parameters are then globally optimized to account for a minimum of flight time (TOF) *and* control effort ($\Delta V = \int |u(t)| dt$ with $|\cdot|$ being the 2-norm). This bi-objective MOP

$$\begin{aligned} & \text{minimize: } \begin{cases} \text{TOF} \\ \Delta V \end{cases} & (14) \\ & \text{subject to: } u \in [0, 800] \text{ mN, } \theta \in [0, 0.4778] \text{ a} \end{aligned}$$

is solved by the subdivision techniques described in Section 2.3. We refer to Section 3.2 for a numerical result. Since merely two parameters are involved the numerical treatment of

such a problem does not represent a challenge for the global optimization method. In fact, we expect that this MOP can as well be solved sufficiently by other state of the art algorithms such as evolutionary multi-objective algorithms (e.g. NSGA-II [Deb et al. (2002)]) which do not require gradient information (note that the gradient of the objectives can ad hoc not be expressed analytically). In case this information can be approximated, methods from mathematical programming can be used such as NBI [Das and Dennis (1998)] or multi-objective continuation methods [Hillermeier (2001)] if the second derivatives are available.

3.2 Optimal control for a fully actuated transfer to L_2

At this stage we consider a more general three-dimensional system that is controlled via three time-dependent translational control forces, one for each degree of freedom of the spacecraft. For our following computations, we use a model involving this more flexible control law and reformulate the system in the context of Lagrangian mechanics.

The Lagrangian corresponding to a spacecraft in the CRTBP reads as

$$L(x, \dot{x}) = \frac{1}{2}m(\dot{x}_1 - \omega x_2)^2 + \frac{1}{2}m(\dot{x}_2 + \omega x_1)^2 + \frac{1}{2}m\dot{x}_3^2 - m\frac{1-\mu}{r_1} - m\frac{\mu}{r_2} \quad (15)$$

with $r_1 = \sqrt{(x_1 + \mu)^2 + x_2^2 + x_3^2}$ and $r_2 = \sqrt{(x_1 - 1 + \mu)^2 + x_2^2 + x_3^2}$. For the angular velocity of the rotating coordinate frame $\omega = 1$ this Lagrangian provides the equations of motions defined in (1) multiplied with the spacecraft mass m . Since the spacecraft is fully actuated, the control forces are simply

$$f(u(t)) = u(t) = (u_x(t), u_y(t), u_z(t)) \in \mathbb{R}^3. \quad (16)$$

According to Section 2.4 the application of the discrete Lagrange-d'Alembert principle provides the forced discrete Euler-Lagrange equations. These serve as equality conditions for minimizing a discrete version of the objective functional according to minimal control effort

$$J(u) = \frac{1}{2} \int_0^T |u(t)|^2 dt, \quad (17)$$

with the final flight time T , and initial and final states $(x(0), \dot{x}(0), x(T), \dot{x}(T))$ as determined in the MOP (14). For simplicity we choose the above measure of control effort $J(u)$ rather than ΔV .

Implementation As a balance between accuracy and efficiency we employ the mid-point rule for approximating the relevant integrals. Correspondingly, we choose a single intermediate control sample for the interval $[t_k, t_{k+1}]$ to be $u_d(t_k + \frac{1}{2}h)$. Although these approximations lead to an optimal control scheme of second order only, the restriction of a maximum time step of $h_{\max} = 10^{-3}$ provides a sufficient accuracy for the scope of our

investigations. The discretization error (order (10^{-6})) is still of two magnitudes smaller than the applied control force (order 10^{-4}).⁷

We start our computations with the step size sequence resulting from the embedded Runge-Kutta scheme used within the global optimization, i.e. rather than using the same step size h for each discrete time interval, our discretization of the Lagrange-d'Alembert principle bases on a sequence of step sizes $\{h_k\}_{k=0}^{N-1}$. Then, the optimal solution trajectories are subsequently refined to provide an initial guess for the optimization with a larger number of discretization points until the desired maximal step size of 10^{-3} is reached. To improve the accuracy of the solutions for future applications, in particular in the presence of path constraints, the use of more sophisticated error based mesh refinement strategies (see e.g. [Betts (2001)]) as well as the use of higher order schemes are recommended and are currently under investigation.

We solve the resulting constrained optimization problem using a sparse SQP optimization algorithm based on SNOPT (see [Gill et al. (1997)] for details) that is implemented in the routine `nag_opt_nlp_sparse` of the NAG library⁸. Here, the numerical tolerances of interest for the feasibility and the optimality of the solutions are 10^{-13} . The gradients of the objective function and the constraints are provided using a numerical approximation by finite differences. In general, software packages for automatic differentiation (e.g. ADOL-C [Walther et al. (1996)]) are recommended to speed up the algorithm.

Results We apply the optimal control scheme to *all* Pareto solutions for the purpose of illustration. Note that, such a computation may be time consuming and, in fact, a strong point of our approach is that the local optimization in principle only must be carried out for *a few* promising Pareto solutions.

Figure 6 illustrates the solutions obtained from the global multi-objective optimization given in (14) applied to the simplified system with constant control (dashed) as well as the solutions resulting from the local single-objective re-optimization with the more flexible control model (denoted by “full system”) described above (solid). For the local optimization the trajectories corresponding to the points on the dashed curve served as initial guesses. These initial guesses consist of the entire state and control trajectories as well as the boundary constraints and the flight time resulting from the solutions of (14). We start the computations with the number of discretization points and the step size lengths corresponding to the solutions of (14). Depending on the flight time, the number of discretization points varies between $N = 40$ and $N = 80$ points for one trajectory. This results into discrete solutions with step sizes h_k varying between $a \cdot 10^{-2}$ and $b \cdot 10^{-5}$, $0 < a, b < 10$. The solution trajectories are refined and the computations restart with more discretization points according to a maximal step size of $\max_k h_k \leq 10^{-2}$ (solid line)

⁷Note that, in the presence of active path constraints the order of accuracy might decrease. However, for our computations we do not take path constraints into account.

⁸<http://www.nag.com>

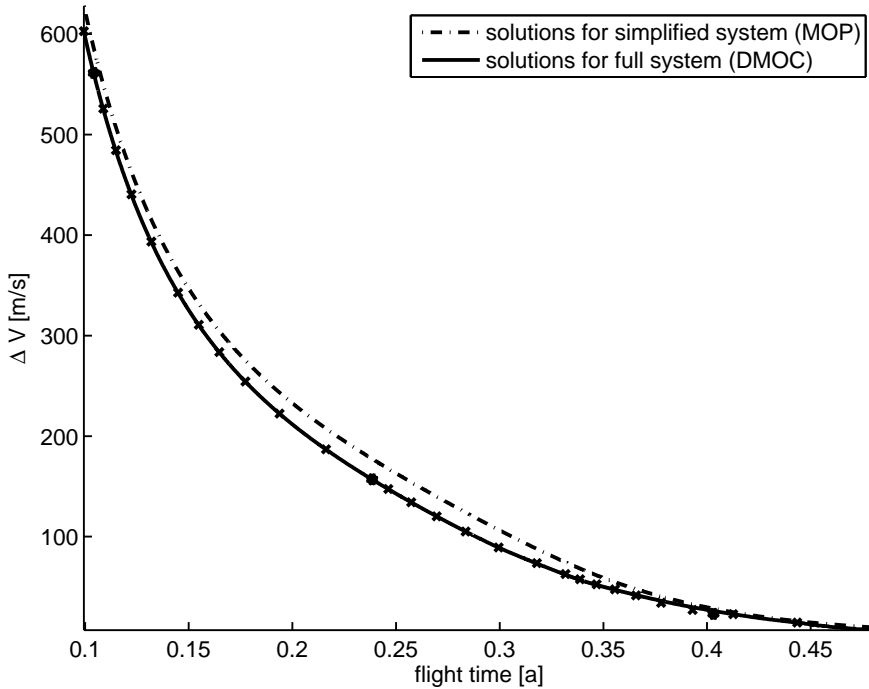


Figure 6: Optimized solutions for the transfer from Earth to a Halo orbit around L_2 . Dashed: Solutions of the global multi-objective optimization problem for the simplified system with objective functions ΔV and flight time T . Solid: Local re-optimization of control effort by DMOC with the full system and fixed flight time for $h_{\max} = 10^{-2}$ and $h_{\max} = 10^{-3}$ (\times). Points: Selected reference trajectories for the formation flight (cf. Figure 7).

and $\max_k h_k \leq 10^{-3}$ (\times).⁹

As the solid curve lies below the dashed one, the ΔV is slightly improved. Dependent on the choice of the trajectory the improvement lies between 4% and 15%. Comparing the results for a maximal step size $h_{\max} = 10^{-2}$ and $h_{\max} = 10^{-3}$ this improvement differs only in 0.1%, confirming that w.r.t. a comparison of the global and local optimal solution the approximation resulting from the underlying discretization grid is reasonable accurate.

In Figure 7 three particular optimal trajectories and controls corresponding to the points in Figure 6 are illustrated. The trajectories start close to Earth (\circ) and end on the Halo orbit (\times). The first trajectory is a relatively time-efficient optimum with a flight time of 0.1042 a and $\Delta V = 561.39$ m/s. On the contrary, the third trajectory is relatively fuel-efficient as indicated by a ΔV of 23.14 m/s but requires a flight time of 0.4031 a. Finally, the second trajectory can be considered as a compromise between short flight time (0.2385 a) and low control effort ($\Delta V = 157.39$ m/s). Here the values of ΔV are

⁹Due to the high computational effort (several hours) we apply the optimization scheme to a smaller number of trajectories for $\max_k h_k \leq 10^{-3}$.

accurate up to 0.01 m/s.

Although the ΔV is slightly improved, the optimal trajectories resulting from the global and the local method look very similar. This is due to the fact that the mission constraints (boundary constraints and flight time) and the initial guess are chosen in exact accordance with the optimal trajectories computed with the global method. Thus, the multi-objective optimization for the restricted model already seems to provide very good initial guesses for the optimal control scheme applied to the more detailed model.

In order to obtain an estimate on how useful the information from the global Pareto optimization is, we repeat the DMOC computations using more naive initial guesses. Here, we still make use of information about the boundary constraints, the flight time, the number of discretization points, and the step size lengths as resulting from (14), but rather than initializing DMOC with the solution trajectories of (14), we choose a straight line connecting the bounds as initial guess and assume the controls to be zero.

The results are illustrated in Figure 8. Although all solutions are feasible, not all trajectories are optimal in the sense that the tolerances for optimality have not been satisfied of the SQP solver. Therefore, the points, where each point represents one solution trajectory, spread out (cf. left of Figure 8). In Figure 8 (right) (zoom of the lower part) we observe that for the trajectories with low flight time a good initial guess is less important since the local optimal control method provides solutions which are as good as those with the better initial guess. For larger flight times, however, the optimal trajectories generated with a naive initial guess require a much higher ΔV , i.e. the SQP solver got stuck in a different local minimum. In Figure 9 the resulting trajectory (solid) with a flight time of $T = 0.34758$ a is depicted which corresponds to the first peak in Figure 8 (right). As opposed to the solutions in Figure 7 this trajectory (solid) obtained with the local solver using a naive initial guess as input differs significantly from the solution obtained by using the good initial guess from the global optimization (dashed). For a fuel efficient transfer, the trajectory of the spacecraft is significantly altered by the low thrust in comparison to the natural dynamics. Consequently, as depicted in Figure 9 (right), this maneuver requires a much higher control effort.

This example indicates that only an entire exploitation of the knowledge gained from a global multi-objective optimization leads to a smooth connected Pareto set and confirms the importance of good initial guesses for the local optimal control scheme.

On the effect of the low-thrust control. Since the applied control force of maximal 800 mN yields an acceleration in the magnitude of 10^{-4} m/s for a 4000 kg spacecraft as assumed in our model, we briefly discuss the effects of such a small continuous control. Figure 10 depicts the three trajectories of Figure 7 (left) with the optimal control obtained by our methods (solid) and the progress of the trajectory if no thrust (i.e. $u = 0$) would be applied (dashed). The initial conditions (start point and integration time) are equal for each controlled trajectory and its uncontrolled analog.

For the third trajectory the non-existence of thrusting causes the spacecraft to ap-

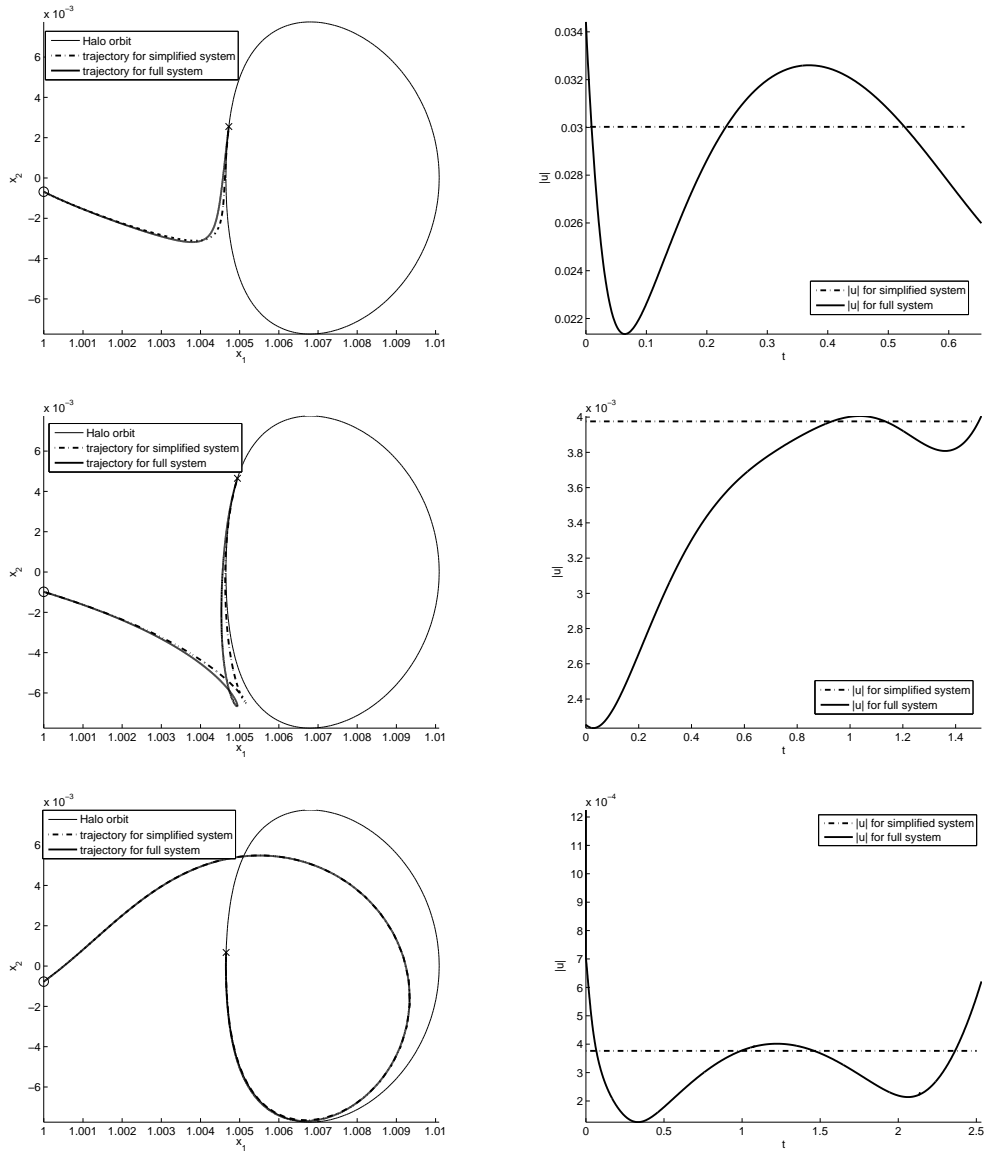


Figure 7: Optimized trajectories and controls for the transfer from a region close to Earth to an L_2 Halo orbit with objective functions ΔV and flight time T . Left: The trajectories start at \circ and end at \times . Right: Time evolution of the 2-norm of the controls. Top: Time-efficient solution ($\Delta V = 561.39$ m/s and $T = 0.1042$ a). Center: Compromise of time and control efficiency ($\Delta V = 157.39$ m/s and $T = 0.2385$ a). Bottom: Fuel-efficient solution ($\Delta V = 23.14$ m/s and $T = 0.4031$ a).

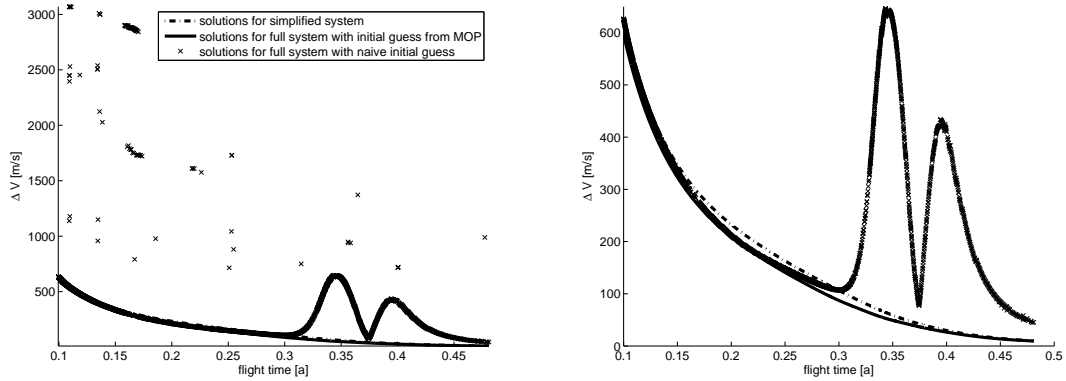


Figure 8: Optimized solutions for the transfer from Earth to an L_2 Halo orbit (Right: Zoom of the lower part). Dashed: Solutions of the multi-objective optimization problem for the simplified system with objective functions ΔV and flight time T . Solid: Solutions of the optimal control problem for the system model with fixed flight time, minimal control effort and initial guesses provided by the MOP. Crosses: Solutions of the optimal control problem for the full system with fixed flight time, minimal control effort and naive initial guesses.

proach but to miss the Halo orbit. In this case, the natural dynamics subsequently takes the spacecraft away from that Halo. Such a behavior can be expected since the thrust allows for a change of the Jacobi constant whereas this magnitude can not change for an uncontrolled trajectory. As a consequence, the controlled trajectory does not follow an invariant manifold of this Halo orbit.

For the upper two pictures of Figure 10 the same effect can be observed when the integration time is increased. Summarized, the effects of the control are not very large but decisive to reach the Halo orbit.

3.3 Reconfiguration of a formation flight

Our next aim (Step 3 of our approach) is the computation of a formation flight of a group of n spacecraft along the precomputed reference trajectories. Here, we are interested in optimal open loop control laws leading to a reconfiguration of the group from an initial configuration into a prescribed target configuration while minimal and maximal distances between the spacecraft have to be fulfilled. For the purpose of this work we restrict ourselves to the unperturbed case. Note that, in light of the tight error tolerances required for formation keeping the computed optimal trajectories have to be stabilized by e.g. suitable feedback laws in order to account for the effects of perturbations.

For the reconfiguration we assume continuous thrust without constraints on the maximal thrust magnitude. We compute the optimal control force $u^{(i)}$, $i = 1, \dots, n$, for each spacecraft, such that the group moves from a given initial state $(x^{(i)}, \dot{x}^{(i)})_{i=1}^n$ into a prescribed target manifold within a given time interval $[0, T]$. Similar computations have been

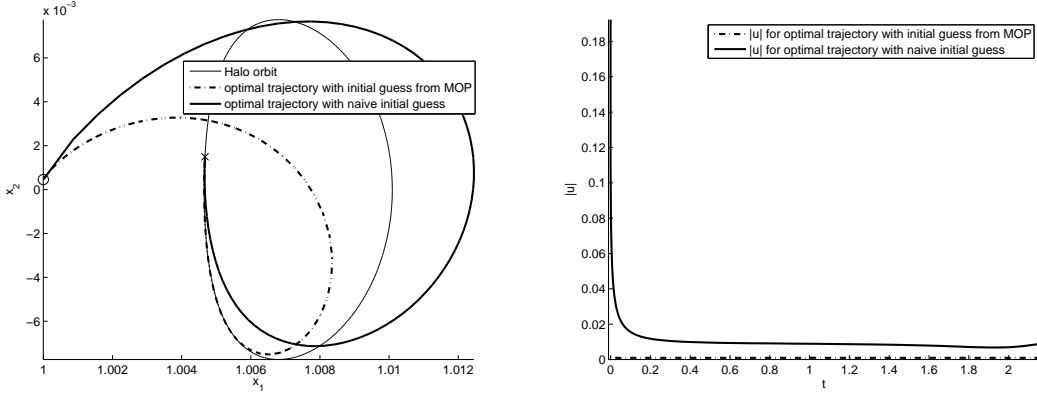


Figure 9: Optimized trajectories and controls for the transfer from a region close to Earth to an L_2 Halo orbit with objective functions ΔV and flight time T (using a naive initial guess for DMOC). Left: The trajectories start at \circ and end at \times . The spacecraft does no longer approach the Halo orbit in a similar way as given by the natural dynamics leading to a much higher control effort as depicted on the right. Right: Time evolution of the 2-norm of the controls.

done in [Dellnitz et al. (2006a), Junge et al. (2006), Junge and Ober-Blöbaum (2005)] where a reconfiguration of a group of spacecraft modeled by rigid bodies along the L_2 Halo orbit was performed. For the purpose of this contribution, we model the spacecraft as point masses. However, the same computations can be performed with the more complex rigid body model. Each spacecraft is described by the same Lagrangian (15) and steered by the same control law (16) assuming that each spacecraft is affected by the same gravitational potential but there is no interaction between the vehicles. We consider $n = 4$ spacecraft as planned for the DARWIN mission and the target manifold is defined by prescribing the relative position of the spacecraft and their common velocity. We additionally require the resulting trajectory to minimize a given objective functional related to the associated fuel consumption of the spacecraft.

More precisely, for the target state, we require the spacecraft to be located on the corners of a square with center on a Halo orbit, where this square is assumed to span a prescribed plane given by its normal $\nu \in \mathbb{R}^3$. The target manifold $Y \subset \mathbb{R}^{24}$ is the set of all states (x, \dot{x}) with $x = (x^{(i)})_{i=1}^4$ and $\dot{x} = (\dot{x}^{(i)})_{i=1}^4$ such that the following conditions are satisfied:

1. The spacecraft are located on the corners of a square of prescribed size and prescribed center M_0 on a fixed Halo orbit, where M_0 is the final point of the reference trajectory computed in Section 3.2. Let $r_0 \in \mathbb{R}$ be a given side length. To ensure the common center of mass to be M_0 we require that

$$h(x) = \frac{1}{4} \sum_{i=1}^4 x^{(i)} - M_0 = 0, \quad (18)$$

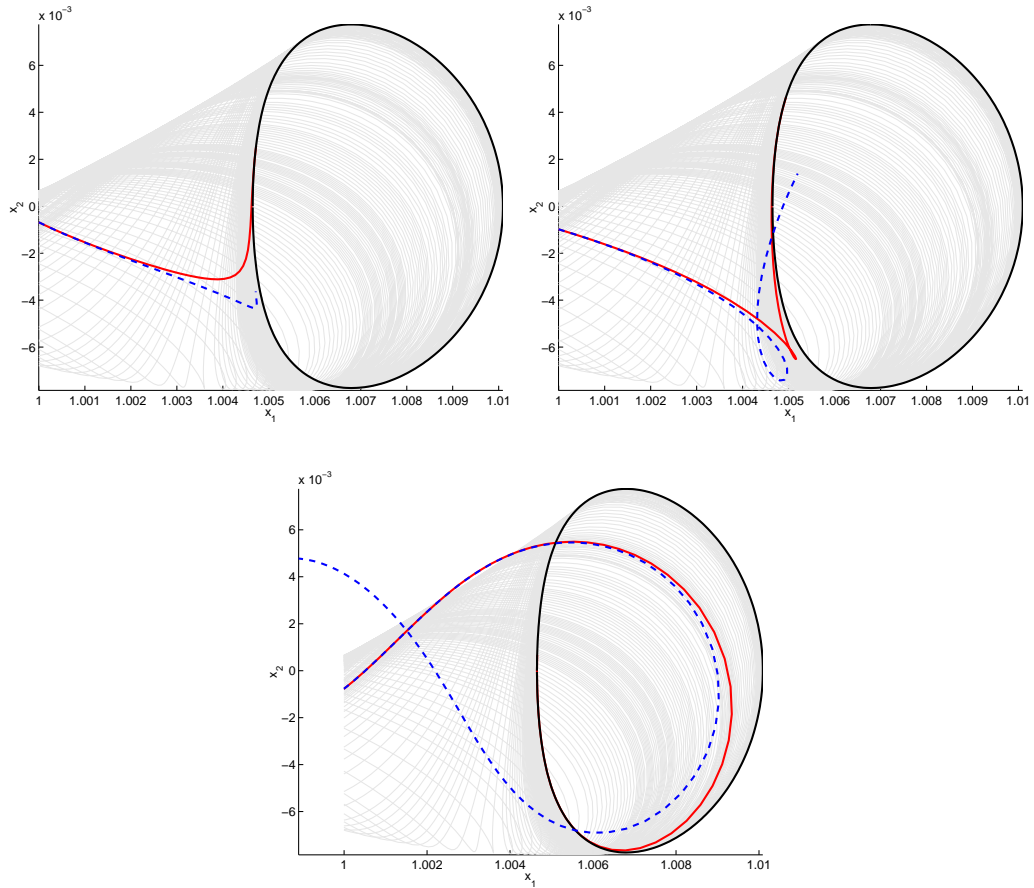


Figure 10: The effect of low-thrust control. Comparison of controlled optimal trajectory of Figure 7 (solid) and the corresponding uncontrolled trajectory with the same start point but $u = 0$ (dashed). Without control the Halo orbit (closed solid line) is missed by the spacecraft. In the first two cases the trajectory moves to the left after some additional integration time.

for a function $h : \mathbb{R}^{12} \rightarrow \mathbb{R}^3$. In addition, we have the constraints

$$k_1(x) = \|x^{(i)} - x^{(j)}\| - r_0 = 0, \quad (i, j) \in \{(1, 2), (2, 3), (3, 4), (4, 1)\}, \quad (19)$$

$$k_2(x) = \|x^{(i)} - x^{(i+2)}\| - \sqrt{2}r_0 = 0, \quad i = 1, 2, \quad (20)$$

with functions $k_j : \mathbb{R}^{12} \rightarrow \mathbb{R}$, $j = 1, 2$, which guarantee an equidistant arrangement to a square with side length r_0 .

2. All spacecraft are in a plane with normal ν . Due to the constraints (18)–(20), the condition

$$l(x) = \langle x^{(i)} - x^{(i+2)}, \nu \rangle = 0, \quad i = 1, 2,$$

for a function $l : \mathbb{R}^{12} \rightarrow \mathbb{R}$ ensures the square formation to span the prescribed plane.

3. All spacecraft have the same prescribed linear velocity, $\dot{x}^{(i)} = \dot{x}_0$, $i = 1, \dots, 4$, where \dot{x}_0 is determined on basis of the Halo orbit under consideration.

Thus, the target manifold is defined by

$$Y = \{(x, \dot{x}) \in \mathbb{R}^{24} \mid h(x) = 0, k_j(x) = 0, l(x) = 0, \dot{x}^{(i)} = \dot{x}_0 \\ \text{with } j = 1, 2 \text{ and } i = 1, \dots, 4\}.$$

As mentioned, in addition to controlling to the target manifold, we would like to minimize the fuel consumption of the spacecraft. Here we consider the objective function

$$J(u) = \sum_{i=1}^4 J_i(u^{(i)}) = \sum_{i=1}^4 \int_0^T |u^{(i)}(t)|^2 dt,$$

where J_i is the objective functional for spacecraft i and $u(t) = (u^{(1)}(t), \dots, u^{(4)}(t))$ denote the control functions for the system.

Collision avoidance For communication reasons the spacecraft are required to keep a prescribed maximal distance d_{\max} to each other during the formation flight. Additionally, collisions between the spacecraft have to be avoided during the reconfiguration which leads to inequality constraints for each time step t_k as

$$d_{\min} \leq \|x^{(i)}(t_k) - x^{(j)}(t_k)\| \leq d_{\max}, \quad i, j = 1, \dots, 4, \quad i \neq j, \quad k = 0, \dots, N. \quad (21)$$

Linearization One major numerical problem in a direct application of the numerical scheme described above (of any scheme, actually) lies in the fact that the scales of interest differ by a factor of around 10^9 : the distance between the Sun and the Earth is of the order of 10^{11} m, while the distances between the spacecraft are of the order of several 100 m. When using standard double-precision floating point arithmetic, rounding errors will notably influence any corresponding computation. On the other hand, we are interested in the relative positions of the spacecraft with respect to each other only.

We therefore perform our computations in a local coordinate system $y = (y_1, y_2, y_3)$ by linearizing the system around a reference trajectory. Let (x_k^R, \dot{x}_k^R) , $k = 1, \dots, N$, be

states of the given reference trajectory (as shown in Figure 7). Writing $y_k = x_k - x_k^R$, the discrete Euler-Lagrange equations (12) for the discrete optimization problem are replaced by their linearization given by

$$D_1 D_2 L_d(x_{k-1}^R, x_k^R) y_{k-1} + D_2 D_2 L_d(x_{k-1}^R, x_k^R) y_k \\ + D_1 D_1 L_d(x_k^R, x_{k+1}^R) y_k + D_2 D_1 L_d(x_k^R, x_{k+1}^R) y_{k+1} + f_{k-1}^+ + f_k^- = 0,$$

for $k = 1, \dots, N-1$, where D_i denotes the derivative w.r.t. the i -th slot. Although we are now faced with a linear optimal control problem with quadratic objective function, we use the optimal control method DMOC for our computations since the path constraints (21) can be incorporated easily.

Results The required control acceleration for the reconfiguration are of the order of approximately 10^{-11} m/s² which may lead to numerical difficulties if the internal tolerances of the SQP algorithm do not allow for tolerances below this level (see for instance [Marchand et al. (2005)]). The linearization and the use of a length dimension of 10^1 m and time dimension of $\frac{1}{2\pi}$ a together with a feasibility and optimality tolerance of 10^{-13} circumvents this numerical issue. In addition, by performing the same numerical steps as for the transfer trajectories, a maximal step size of 10^{-3} leads to a precision of 10^{-5} m for the relative position of the spacecraft within the formation, which is sufficient for the aim of buliding up a desired formation around the Halo orbit. However, for station keeping and interferometry this accuracy has to be increased by the use of smaller step sizes or higher order schemes.

For each of the three re-optimized trajectories depicted in Figure 7 we compute a formation flight along these trajectories. For our computations we choose a minimal spacecraft distance $d_{\min} = 5$ m and a maximal distance $d_{\max} = 50$ m. All spacecraft start in a line on the y_1 -axis with a distance of 15 m from each other. At the end they form up a square with side length of 30 m. In Figure 11 the relative trajectories of each spacecraft for the different reference trajectories are illustrated. Here, the reference trajectories are located in the coordinate origin (0,0,0). For the time-efficient trajectory and the trajectory representing a compromise between time- and fuel-efficiency the solutions for each spacecraft look similar (see Figure 11 (a) and (b)), anyhow the time-efficient formation flight requires a higher ΔV of $2.1203 \cdot 10^{-3}$ m/s compared to the $\Delta V = 7.6457 \cdot 10^{-4}$ m/s required for the compromise trajectory. However, for the formation flight along the fuel-efficient trajectory we have an even higher $\Delta V = 2.6849 \cdot 10^{-3}$ m/s as indicated by Figure 11 (c). The single spacecraft trajectories spiral around the reference trajectory before they form up the final desired configuration.

The ΔV required additionally for the formation control is almost negligible compared to the ΔV for the transfer from Earth to L_2 . Thus, a space mission designer may base the first decision on suitable trajectories only on the data of the reference trajectories.

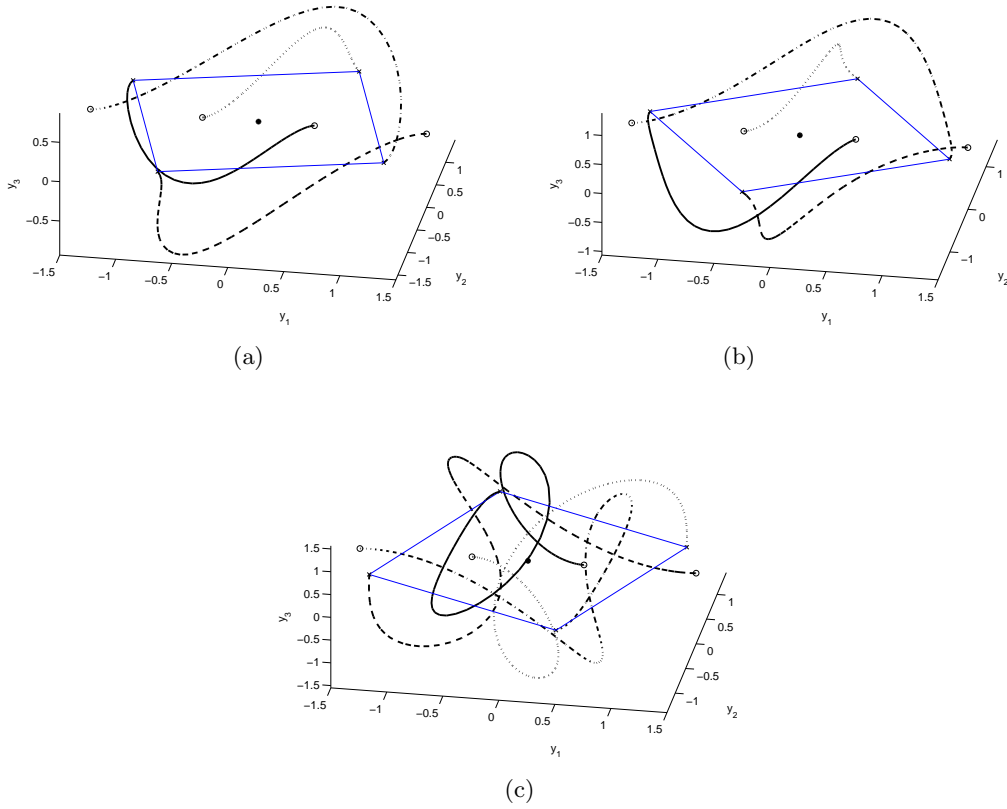


Figure 11: Relative trajectories of four spacecraft flying in formation along the three reference trajectories (located in $(0,0,0)$) depicted in Figure 7. The formation starts in a line with a distance of 15 m from each other (\circ) and ends in a square with side length of 30 m (\times). (a) Formation flight along a time-efficient transfer trajectory (additional $\Delta V = 2.1203 \cdot 10^{-3}$ m/s). (b) Formation flight along a time- and fuel-efficient transfer trajectory (additional $\Delta V = 7.6457 \cdot 10^{-4}$ m/s). (c) Formation flight along a fuel-efficient transfer trajectory (additional $\Delta V = 2.6849 \cdot 10^{-3}$ m/s).

4 Conclusion and future work

Conclusion In this article we have described an efficient strategy of finding low thrust spacecraft trajectories which are optimal with respect to flight time *and* ΔV . We have also presented how to utilize these optimal compromises as reference trajectories for a formation flight. Particularly, we want to stress that not only fixed end points but also manifold constraints on the formation can be solved by employing the recently developed method DMOC. In summary, we applied the following three-stage approach: We performed a multi-objective optimization by a set-oriented subdivision technique, then we refined the resulting trajectories by the local optimal control method DMOC, and finally, we obtained several trajectories for the formation using DMOC again.

Our detailed numerical study documents that the preselection of trajectories by a global method with a yet simple control law substantially contributes to the quality of solutions obtained by the local method (Sections 3.2 and 3.3). In particular, the comparison of trajectories resulting from local optimization with different initial guesses indicate that only the exploitation of the full knowledge gained from the global multi-objective optimization leads to satisfactory results. A further observation is that the changes in ΔV and flight time introduced by the local re-optimization do not influence the qualitative picture of the Pareto set too much and that the additional ΔV for the formation flight is almost negligible with respect to the total one. This legitimates a posteriori the division into three separate steps and illustrates that the knowledge of the *entire* Pareto set in the first step can already help mission designers to decide which optimal compromise to take.

Future work A goal for future work is to even more improve the solution trajectories with respect to a lower ΔV and shorter flight times at the first stage. The issue here is to find a compromise between the fast calculation of the global Pareto set and obtaining trajectories closer to the locally optimized ones. The trade-off is directly reflected in the number of parameters in the global multi-objective optimization which can easily be enlarged by considering more complex control laws, i.e. control functions which are parametrized by a higher number of parameters by choosing e.g. piecewise constant instead of constant controls. In addition, rather than fixing one Halo orbit for the destination of the spacecraft, a further parameter would let the entire family of Halo orbits be subject to optimization.

Methodically, it is of great interest to combine both approaches in a more intertwined way to directly compute global Pareto-optimal solutions for optimal control problems within the *detailed* model. The key point is here that the use of two different models for the global and local optimization would not be necessary any longer. In this way, the mission designer could base his or her decision on the final solution instead of an intermediate result.

Acknowledgements

This research was partly supported by the EU funded Marie Curie Research Training Network *AstroNet*, by the AFOSR grant FA9550-08-1-0173, and by the priority program SPP 1305 of the Deutsche Forschungsgemeinschaft (DFG).

References

- [Abraham and Marsden (1978)] Abraham, R. and Marsden, J.E.: 1978, *Foundations of Mechanics*, Second Edition, Addison-Wesley.
- [Baig and McInnes (2009)] Baig, S. and McInnes, C.R.: 2009, 'Artificial halo orbits for low-thrust propulsion spacecraft', *Celestial Mechanics and Dynamical Astronomy* 104, 321-335.
- [Barden et al. (1997)] Barden, B.T., Howell, K.C. and Lo, M.W.: 1997, 'Applications of dynamical systems theory to trajectory design for a libration point mission', *Journal of the Astronautical Science* 45(2), 161-178.
- [Belbruno (2004)] Belbruno, E.: 2004, *Capture Dynamics and Chaotic Motions in Celestial Mechanics*, Princeton University Press.
- [Belbruno and Marsden (1997)] Belbruno, E. and Marsden, B.: 1997, 'Resonance hopping in comets', *The Astronomical Journal* 113(4), 1433-1444.
- [Belbruno and Miller (1993)] Belbruno, E. and Miller, J.: 1993, 'Sun-perturbed Earth-to-Moon transfers with ballistic capture', *Journal of Guidance, Control, and Dynamics* 16, 770-775.
- [Betts (2001)] Betts, J.T.: 2001, 'Practical Methods for Optimal Control Using Nonlinear Programming', *Advances in Design and Control. Society for Industrial and Applied Mathematics*, 2 edition, Philadelphia, PA.
- [Betts (1998)] Betts, J.T.: 1998, 'Survey of numerical methods for trajectory optimization', *AIAA J. Guidance, Control, and Dynamics* 21(2), 193-207.
- [Biegler (1984)] Biegler, L.T.: 1984, 'Solution of dynamic optimization problems by successive quadratic programming and orthogonal collocation', *Computers and Chemical Engineering* 8, 243-248.
- [Binder et al. (2001)] Binder, T., Blank, L., Bock, H.G., Bulirsch, R., Dahmen, W., Diehl, M., Kronseder, T., Marquardt, W., Schlöder, J.P. and von Stryk, O.: 2001, 'Introduction to model based optimization of chemical processes on moving horizons', Ed.: M. Grötschel, S.O. Krumke and J. Rambau, In *Online Optimization of Large Scale Systems: State of the Art*, 295-340, Springer.
- [Bock and Plitt (1984)] Bock, H.G. and Plitt, K.J.: 1984, 'A multiple shooting algorithm for direct solution of optimal control problems', *Proc. of 9th IFAC World Congress*, Budapest, 242-247.
- [Coello Coello et al. (2007)] Coello Coello, C., Lamont, G. and Van Veldhuizen, D.: 2007, *Evolutionary Algorithms for Solving Multi-Objective Problems*, Springer, New York.
- [Colonus and Kliemann (2000)] Colonus, F. and Kliemann, W.: 2000, *The dynamics of control*, Birkhäuser, Boston.
- [Conway et al. (2007)] Conway, B.A., Chilan, Ch.M. and Wall, B.J.: 2007, 'Evolutionary principles applied to mission planning problems', *Celestial Mechanics and Dynamical Astronomy* 97, 73-86.
- [Coverstone-Carroll et al. (2000)] Coverstone-Carroll, V., Hartman, J.W. and Mason, W.M.: 2000, 'Optimal Multi-Objective Low-Thrust Spacecraft Trajectories', *Computer Methods in Applied Mechanics and Engineering* 186, 387-402.
- [Das and Dennis (1998)] Das, I., and Dennis, J.: 1998, 'Normal-Boundary Intersection: A New Method for Generating the Pareto Surface in Nonlinear Multicriteria Optimization Problems', *SIAM Journal of Optimization*, 8, 631-657.
- [Deb (2001)] Deb, K.: 2001, *Multi-Objective Optimization Using Evolutionary Algorithms*, Wiley.
- [Deb et al. (2002)] Deb, K., Pratap, A., Agarwal, S., and Meyarivan, T.: 2002, 'A Fast and Elitist Multiobjective Genetic Algorithm: NSGA-II', *IEEE Transactions on Evolutionary Computation*, 6(2), 182-197.

- [Dellnitz et al. (2006a)] Dellnitz, M., Junge, O., Krishnamurthy, A., Ober-Blöbaum, S., Padberg, K. and Preis, R.: 2006, 'Efficient control of formation flying spacecraft', Ed.: F. Meyer auf der Heide and B. Monien, In *New Trends in Parallel & Distributed Computing*, 235-247, Heinz Nixdorf Institut Verlags-schriftreihe.
- [Dellnitz et al. (2001)] Dellnitz, M., Junge, O., Lo, M.W. and Thiere, B.: 2001, 'On the detection of energetically efficient trajectories for spacecraft', *AAS/AIAA Astrodynamics Specialist Conference*, Quebec City, Paper AAS 01-326.
- [Dellnitz et al. (2006b)] Dellnitz, M., Junge, O., Post, M. and Thiere, B.: 2006, 'On target for Venus—set oriented computation of energy efficient low thrust trajectories', *Celestial Mechanics & Dynamical Astronomy*, 95, 357-370.
- [Dellnitz et al. (2005)] Dellnitz, M., Schütze, O. and Hestermeyer, T.: 2005, 'Covering Pareto Sets by Multilevel Subdivision Techniques', *Journal of Optimization Theory and Applications* 124, 113-155.
- [Dellnitz et al. (2002)] Dellnitz, M., Schütze, O. and Sertl, St.: 2002, 'Finding Zeros by Multilevel Subdivision Techniques', *IMA Journal of Numerical Analysis* 22(2), 167-185.
- [Deuffhard (1974)] Deuffhard, P.: 1974, 'A modified Newton method for the solution of ill-conditioned systems of nonlinear equations with application to multiple shooting', *Numerische Mathematik* 22, 289-315.
- [Dichmann et al. (2003)] Dichmann, D.J., Doedel, E.J. and Paffenroth, C.: 2003, 'The Computation of Periodic Solutions of the 3-Body Problem using the Numerical Continuation Software AUTO', *International Conference on Libration Point Orbits and Applications*, 489-528, World Scientific.
- [Farquhar (1970)] Farquhar, R.W.: 1970, 'The control and use of Libration-Point satellites', *NASA TR R-346*.
- [Fliege and Svaiter (2000)] Fliege, J., and Svaiter, B. F.: 2000, 'Steepest descent methods for multicriteria optimization', *Mathematical Methods of Operations Research* 51 (3), 479-494.
- [Garcia and Gómez (2007)] Garcia, F. and Gómez, G.: 2007, 'A note on weak stability boundaries', *Celestial Mechanics and Dynamical Astronomy* 97, 87-100.
- [Gawlik et al. (2009)] Gawlik, E.S., Marsden, J.E., Du Toit, P.C. and Campagnola, S.: 2009, 'Lagrangian coherent structures in the planar elliptic restricted three-body problem', *Celestial Mechanics and Dynamical Astronomy* 103, 227-249.
- [Gerthsen and Vogel (1993)] Gerthsen, Ch. and Vogel, H.: 1993, *Physik*, Springer.
- [Gill et al. (2000)] Gill, P.E., Jay, L.O., Leonard, M.W., Petzold, L.R. and Sharma, V.: 2000, 'An SQP method for the optimal control of large-scale dynamical systems', *J. Comp. Appl. Math* 20, 197-213.
- [Gill et al. (1997)] Gill, P.E., Murray, W. and Saunders, M.A.: 1997, 'SNOPT: An SQP algorithm for large-scale constrained optimization', Report NA 97-2, Department of Mathematics, University of California, San Diego, CA, USA.
- [Gómez et al. (2001)] Gómez, G., Koon, W.S., Lo, M.W., Marsden, J.E., Masdemont, J. and Ross, S.D.: 2001, 'Invariant manifolds, the spatial three-body problem and space mission design', *Advances in the Astronautical Sciences* 109(1), Paper AAS 01-301, 3-22.
- [Hairer et al. (1993)] Hairer, E., Nørsett, S. P. and Wanner, G.: 1993, *Solving ordinary differential equations I*, Springer, Berlin.
- [Han (1976)] Han, S.P.: 1976, 'Superlinearly convergent variable-metric algorithms for general nonlinear programming problems', *Mathematical Programming* 11, 263-282.
- [Hicks and Ray (1971)] Hicks, G. and Ray, W.: 1971, 'Approximation methods for optimal control systems', *Can. J. Chem. Engng.* 49, 522-528.
- [Hillermeier (2001)] Hillermeier, C.: 2001, *Nonlinear Multiobjective Optimization - A Generalized Homotopy Approach*, Birkhäuser, Berlin.
- [Howell et al. (1997)] Howell, K., Barden, B. and Lo, M.W.: 1997, 'Application of Dynamical Systems Theory to Trajectory Design for a Libration Point Mission', *Journal of the Astronautical Sciences* 45(2), 161-178.
- [Howell and Marchand (2003)] Howell, K.C. and Marchand, B.G.: 2003, 'Control Strategies for Formation Flight in the Vicinity of the Libration Points', *AIAA/AAS Space Flight Mechanics Conference*, Ponce, Puerto Rico, AAS Paper 03-113.

- [Junge et al. (2002)] Junge, O., Levenhagen, J., Seifried, A., Dellnitz, M. and Astrium GmbH: 2002, 'Identification of Halo orbits for energy efficient formation flying', *Proc. of the International Symposium Formation Flying*, Toulouse.
- [Junge et al. (2005)] Junge, O., Marsden, J.E. and Ober-Blöbaum, S.: 2005, 'Discrete mechanics and optimal control', *Proc. of 16th IFAC World Congress*, Prague.
- [Junge et al. (2006)] Junge, O., Marsden, J.E. and Ober-Blöbaum, S.: 2006, 'Optimal reconfiguration of formation flying spacecraft - a decentralized approach', *Proc. of IEEE Conference on Decision and Control and European Control Conference ECC*, San Diego, California.
- [Junge and Ober-Blöbaum (2005)] Junge, O. and Ober-Blöbaum, S.: 2005, 'Optimal reconfiguration of formation flying satellites', *Proc. of the IEEE Conference on Decision and Control and European Control Conference ECC*, Seville.
- [Kanso and Marsden (2005)] Kanso, E. and Marsden, J.E.: 2005, 'Optimal motion of an articulated body in a perfect fluid', In *Proc. of the IEEE Conference on Decision and Control and European Control Conference ECC*, Seville.
- [Kechichian (2002)] Kechichian, J.A.: 2002, 'Local Regularization of the Restricted Elliptic Three-Body Problem in Rotating Coordinates', *Journal of Guidance, Control, and Dynamics* 25(6), 1064-1072.
- [Kobilarov et al.(2007)] Kobilarov, M., Desbrun, M., Marsden, J.E. and Sukhatme, G.S.: 2007, 'A discrete geometric optimal control framework for systems with symmetries', *Robotics: Science and Systems* 3, 1-8.
- [Koon et al. (1999)] Koon, W.S., Lo, M.W., Marsden, J.E. and Ross, S.D.: 1999, 'The Genesis Trajectory and Heteroclinic Connections', *AAS/AIAA Astrodynamics Specialist Conference*, Girdwood, Alaska, AAS99-451.
- [Koon et al. (2000)] Koon, W.S., Lo, M.W., Marsden, J.E. and Ross, S.D.: 2000, 'Heteroclinic connections between periodic orbits and resonance transitions in celestial mechanics', *Chaos* 10, 427-469.
- [Koon et al. (2001)] Koon, W.S., Lo, M.W., Marsden, J.E. and Ross, S.D.: 2001, 'Low energy transfer to the Moon', *Celestial Mechanics and Dynamical Astronomy* 81, 63-73.
- [Kraft (1985)] Kraft, D.: 1985, 'On converting optimal control problems into nonlinear programming problems', Ed.: K. Schittkowsky, In *Computational Mathematical Programming*, F15, 261-280, NATO ASI series, Springer.
- [Lee et al. (2005)] Lee, S., von Allmen, P., Fink, W., Petropoulos, A. E., and Terrile, R. J.: 2005, 'Multi-Objective Evolutionary Algorithms for Low-Thrust Orbit Transfer Optimization', Genetic and Evolutionary Computation Conference (GECCO 2005).
- [Leineweber et al. (2003)] Leineweber, D., Bauer, I., Bock, H. and Schlöder, J.: 2003, 'An efficient multiple shooting based reduced SQP strategy for large-scale dynamic process optimization. Part I: Theoretical aspects', *Comp. Chem. Eng.* 27, 157-166.
- [Leiva and Briozzo (2008)] Leiva, A.M. and Briozzo, C.B.: 2008, 'Extension of fast periodic transfer orbits from the Earth-Moon RTBT to the Sun-Earth-Moon Quasi-Bicircular Problem', *Celestial Mechanics and Dynamical Astronomy* 101, 225-245.
- [Leyendecker et al. (2007)] Leyendecker, S., Ober-Blöbaum, S., Marsden, J.E. and Ortiz, M.: 2007, 'Discrete mechanics and optimal control for constrained multibody dynamics', In *Proc. of the 6th International Conference on Multibody Systems, Nonlinear Dynamics, and Control, ASME International Design Engineering Technical Conferences*, Las Vegas, Nevada.
- [Maddock and Vasile (2008)] Maddock C., Vasile M.: 2008, 'Design of Optimal Spacecraft-Asteroid Formations Through a Hybrid Global Optimization Approach', *International Journal of Intelligent Computing and Cybernetics* 1 (2), 239-268.
- [Marchand et al. (2005)] Marchand, B.G., Howell, K.C., and Betts, J.T.: 2005, 'Discrete Optimal Control of S/C Formations Near the L1 and L2 Points of the Sun-Earth/Moon system', *AIAA/AAS Astrodynamics Specialist Conference*, Lake Tahoe, California.
- [Marchand and Howell (2003)] Marchand, B.G. and Howell, K.C.: 2003, 'Formation Flight Near L2 in the Sun-Earth/Moon Ephemeris System Including Solar Radiation Pressure', *AIAA/AAS Astrodynamics Specialist Conference*, Big Sky, Montana, AAS Paper 03-596.
- [Marsden and West (2001)] Marsden, J.E. and West, M.: 2001, 'Discrete mechanics and variational integrators', *Acta Numerica* 10, 357-514.

- [McGehee (1969)] McGehee, R.P.: 1969, 'Some homoclinic orbits for the restricted 3-body problem', PhD Dissertation, University of Wisconsin.
- [Meyer and Hall (1992)] Meyer, K.R. and Hall, R.: 1992, *Hamiltonian Mechanics and the n-body Problem*, Springer, New York.
- [Miettinen (1999)] Miettinen, K.: 1999, *Nonlinear Multiobjective Optimization*, Kluwer Academic Publishers.
- [Mingotti et al. (2009)] Mingotti, G., Topputo, F. and Bernelli-Zazzera, F.: 2009, 'Low-energy, low-thrust transfers to the Moon', To appear in *Celestial Mechanics and Dynamical Astronomy* 105.
- [Ober-Blöbaum (2008)] Ober-Blöbaum, S.: 2008, 'Discrete mechanics and optimal control', PhD Dissertation, University of Paderborn, Paderborn.
- [Pareto (1971)] Pareto, V.: 1971, *Manual of Political Economy*, The MacMillan Press. (original edition in French in 1917)
- [Pergola et al. (2009)] Pergola, P., Geurts, K., Casaregola, C. and Andrenucci, M.: 2009, 'Earth-Mars halo to halo low thrust manifold transfers', To appear in *Celestial Mechanics and Dynamical Astronomy* 105.
- [Powell (1978)] Powell, M.J.D.: 1978, 'A fast algorithm for nonlinearly constrained optimization calculations', Ed.: G.A. Watson, In *Numerical Analysis*, 630, 261-280, Lecture Notes in Mathematics, Springer.
- [Richardson (1980)] Richardson, D.L.: 1980, 'Analytic construction of periodic orbits about the collinear points', *Celestial Mechanics and Dynamical Astronomy* 22(3), 241-253.
- [Schütze et al. (2003)] Schütze, O., Mostaghim, S., Dellnitz, M. and Teich, J.: 2003, 'Covering Pareto Sets by Multilevel Evolutionary Subdivision Techniques', Ed.: C.M. Fonseca, P.J. Fleming, E. Zitzler, K. Deb and L. Thiele, In *Evolutionary Multi-Criterion Optimization*, Lecture Notes in Computer Science.
- [Schütze et al. (2008a)] Schütze, O., Jourdan, L., Legrand, T., Talbi, E.G. and Wojkiewicz, J.L.: 2008, 'New Analysis of the Optimization of Electromagnetic Shielding Properties Using Conducting Polymers and a Multi-Objective Approach', *Polymers for Advanced Technologies* 19, 762-769.
- [Schütze et al. (2008b)] Schütze, O., Vasile, M., Junge, O., Dellnitz, M. and Izzo, D.: 2008, 'Designing optimal low thrust gravity assist trajectories using space pruning and a multi-objective approach', *Engineering Optimization* 41(2), 155-181.
- [Schütze et al. (2008c)] Schütze, O., Vasile, M., Coello Coello, C. A.: 2008, 'Approximate Solutions in Space Mission Design', *Parallel Problem Solving from Nature (PPSN 2008)*, 805-814.
- [Stoer and Bulirsch (1993)] Stoer, J. and Bulirsch, R.: 1993, *Introduction into numerical analysis*, Springer.
- [Szebehely (1967)] Szebehely, V.: 1967, *Theory of Orbits*, Academic Press, New York, London.
- [Tang and Conway (1995)] Tang, S. and Conway, B.A.: 1995, 'Optimization of Low-Thrust Interplanetary Trajectories Using Collocation and Nonlinear Programming', *Journal of Guidance, Control, and Dynamics* 18(3), 599-604.
- [Vasile et al. (2006)] Vasile, M., Schütze, O., Junge, O., Radice, G. and Dellnitz, M.: 2006, 'Spiral trajectories in global optimisation of interplanetary and orbital transfers', Technical report, Ariadna Study Report AO4919 05/4106, Contract Number 19699/NL/HE, European Space Agency.
- [Vasile (2009)] Vasile, M.: 2009, 'Hybrid behavioral-based multiobjective space trajectory optimization', *Multi-Objective Memetic Algorithms Series: Studies in Computational Intelligence* 171, 231-254.
- [Vavrina and Howell (2008)] Vavrina, M. A., and Howell, K. C.: 2008, 'Global Low-Thrust Trajectory Optimization through Hybridization of a Genetic Algorithm and a Direct Method', AIAA/AAS Astrodynamics Specialist Conference, AIAA 2008-6614.
- [von Stryk (1993)] von Stryk, O.: 1993, 'Numerical solution of optimal control problems by direct collocation', Ed.: R. Bulirsch, A. Miele, J. Stoer and K.H. Well, In *Optimal Control - Calculus of Variation, Optimal Control Theory and Numerical Methods*, 111, 129-143, International Series of Numerical Mathematics, Birkhäuser.
- [Walther et al. (1996)] Walther, A., Kowarz, A. and Griewank, A.: 1996, 'ADOL-C: a package for the automatic differentiation of algorithms written in C/C++', *ACM TOMS* 22(2):131-167.